Combined microfluidic-optical DNA analysis with single-base-pair sizing capability

MARKUS POLLNAU,[1,2,*] MANFRED HAMMER,[1,3] CHAITANYA DONGRE,[1] AND HUGO J. W. M. HOEKSTRA[1]

[1]*Integrated Optical Microsystems Group, MESA+ Institute for Nanotechnology, University of Twente, P. O. Box 217, 7500 AE Enschede, The Netherlands*
[2]*Department of Materials and Nano Physics, School of Information and Communication Technology, KTH−Royal Institute of Technology, Electrum 229, Isafjordsgatan 22−24, 16440 Kista, Sweden*
[3]*Theoretical Electrical Engineering, University of Paderborn, Warburger Strasse 100, 33098 Paderborn, Germany*
*m.pollnau@utwente.nl

Abstract: DNA sequencing by microchip capillary electrophoresis (CE) enables cheap, high-speed analysis of low reagent volumes. One of its potential applications is the identification of genomic deletions or insertions associated with genetic illnesses. Detecting single base-pair insertions or deletions from DNA fragments in the diagnostically relevant size range of 150–1000 base-pairs requires a variance of $\sigma^2 < 10^{-3}$. In a microfluidic chip post-processed by femtosecond-laser writing of an optical waveguide we CE-separated 12 blue-labeled and 23 red-labeled DNA fragments in size. Each set was excited by either of two lasers power-modulated at different frequencies, their fluorescence detected by a photomultiplier, and blue and red signals distinguished by Fourier analysis. We tested different calibration strategies. Choice of the fluorescent label as well as the applied fit function strongly influence the obtained variance, whereas fluctuations between two consecutive experiments are less detrimental in a laboratory environment. We demonstrate a variance of $\sigma^2 \approx 4\times10^{-4}$, lower than required for the detection of single base-pair insertion or deletion in an optofluidic chip.

OCIS codes: (130.3120) Integrated optics devices; (170.3890) Medical optics instrumentation.

References and links

1. A. Manz, N. Graber, and H. M. Widmer, "Miniaturized total chemical analysis systems: a novel concept for chemical sensing," *Sens. Actuator B–Chem.* **1**(1-6), 244–248 (1990).
2. R. D. Reyes, D. Iossifidis, P. A. Auroux, and A. Manz, "Micrototal analysis systems 1. Introduction, theory, and technology," *Anal. Chem.* **74**(12), 2623–2636 (2002).
3. P. A. Auroux, D. R. Reyes, D. Iossifidis, and A. Manz, "Micrototal analysis systems 2. Analytical standard operations and applications," *Anal. Chem.* **74**(12), 2637–2652 (2002).
4. D. J. Harrison, K. Fluri, K. Seiler, Z. H. Fan, C. S. Effenhauser, and A. Manz, "Micromachining a miniaturized capillary electrophoresis based chemical analysis system on a chip," *Science* **261**(5123), 895–897 (1993).
5. G. J. M. Bruin, "Recent developments in electrokinetically driven analysis on microfabricated devices," *Electrophoresis* **21**(18), 3931–3951 (2000).
6. J. P. Landers, "Molecular diagnostics on electrophoretic microchips: a review," *Anal. Chem.* **75**(12), 2919–2926 (2003).
7. International Human Genome Sequencing Consortium, "Initial sequencing and analysis of the human genome," *Nature* **409**(6822), 860–921 (2001).
8. G. W. Slater, M. Kenward, L. C. McCormick, M. G. Gauthier, "The theory of DNA separation by capillary electrophoresis," *Current Opinion Biotechnol.* **14**(1), 58–64 (2003).
9. D. Altshuler, M. J. Daly, and E. S. Lander, "Genetic mapping of human disease," *Science* **322**(5903), 881–888 (2008).
10. C. P. Fredlake, D. G. Hert, C. W. Kan, T. N. Chiesl, B. E. Root, R. E. Forster, and A. E. Barron, "Ultrafast DNA sequencing on a microchip by a hybrid separation mechanism that gives 600 bases in 6.5 minutes," *Proc. Natl. Acad. Sci. USA* **105**(2), 476–481 (2008).
11. J. Eid, A. Fehr, J. Gray, K. Luong, J. Lyle, G. Otto, P. Peluso, D. Rank, P. Baybayan, B. Bettman, A. Bibillo, K. Bjornson, B. Chaudhuri, F. Christians, R. Cicero, S. Clark, R. Dalal, A. Dewinter, J. Dixon, M. Foquet, A. Gaertner, P. Hardenbol, C. Heiner, K. Hester, D. Holden, G. Kearns, X. Kong, R. Kuse, Y. Lacroix, S. Lin, P. Lundquist, C. Ma, P. Marks, M. Maxham, D. Murphy, I. Park, T. Pham, M. Phillips, J. Roy, R. Sebra, G. Shen,

J. Sorenson, A. Tomaney, K. Travers, M. Trulson, J. Vieceli, J. Wegener, D. Wu, A. Yang, D. Zaccarin, P. Zhao, F. Zhong, J. Korlach, and S. Turner, "Real-time DNA sequencing from single polymerase molecules," *Science* **323**(5910), 133–138 (2009).
12. D. Pile, "Eavesdropping on DNA replication," *Nat. Photonics* **3**(2), 79–80 (2009).
13. Pacific Biosciences, 2016. http://www.pacificbiosciences.com.
14. E. T. Lagally and R. A. Mathies, "Integrated genetic analysis Microsystems," *J. Phys. D: Appl. Phys.* **37**(23), 245–261 (2004).
15. C. J. Easley, J. M. Karlinsey, J. M. Bienvenue, L. G. Legendre, M. G. Roper, S. H. Feldman, M. A. Hughes, E. L. Hewlett, T. J. Merkel, J. P. Ferrance, and J. P. Landers, "A fully integrated microfluidic genetic analysis system with sample-in-answer-out capability," *Proc. Natl. Acad. Sci. USA* **103**(51), 19272–19277 (2006).
16. C. Dongre, M. Pollnau, and H. J. W. M. Hoekstra, "All-numerical noise filtering of fluorescence signals for achieving ultra-low limit of detection in biomedical applications," *Analyst* **136**(6), 1248–1251 (2011).
17. E. Verpoorte, "Chip vision – optics for microchips," Lab Chip **3**(3), 42–52 (2003).
18. Y. Bellouard, A. Said, M. Dugan, and P. Bado, "Monolithic three-dimensional integration of micro-fluidic channels and optical waveguides in fused silica," *Mater. Res. Soc. Symp. Proc.* **782**, A3.2.1–A3.2.6 (2004).
19. D. B. Wolfe, D. V. Vezenov, B. T. Mayers, G. M. Whitesides, R. S. Conroy, and M. G. Prentiss, "Diffusion controlled optical elements for optofluidics," *Appl. Phys. Lett.* **87**(18), 181105 (2005).
20. R. W. Applegate Jr., J. Squier, T. Vestad, J. Oakey, D. W. M. Marr, P. Bado, M. A. Dugan, and A. A. Said, "Microfluidic sorting system based on optical waveguide integration and diode laser bar trapping," *Lab Chip* **6**(3), 422–426 (2006).
21. D. Psaltis, S. R. Quake, and C. Yang, "Developing optofluidic technology through the fusion of microfluidics and optics," *Nature* **442**(7101), 381–386 (2006).
22. S. Götz and U. Karst, "Recent developments in optical detection methods for microchip separations," *Anal. Bioanal. Chem.* **387**(1), 183–192 (2007).
23. D. Yin, E. J. Lunt, M. I. Rudenko, D. W. Deamer, A. R. Hawkins, and H. Schmidt, "Planar optofluidic chip for single particle detection, manipulation, and analysis," *Lab Chip* **7**(9), 1171–1175 (2007).
24. H. C. Hunt and J. S. Wilkinson, "Optofluidic integration for microanalysis," *Microfluid. Nanofluid.* **4**(1-2), 53–79 (2008).
25. F. B. Myers and L. P. Lee, "Innovations in optical microfluidic technologies for point-of-care diagnostics," *Lab Chip* **8**(12), 2015–2031 (2008).
26. R. Martínez Vázquez, R. Osellame, D. Nolli, C. Dongre, H. H. van den Vlekkert, R. Ramponi, M. Pollnau, and G. Cerullo, "Integration of femtosecond laser written optical waveguides in a lab-on-chip," *Lab Chip* **9**(1), 91–96 (2009).
27. A. Crespi, Y. Gu, B. Ngamson, H. J. W. M. Hoekstra, C. Dongre, M. Pollnau, R. Ramponi, H. H. van den Vlekkert, P. Watts, G. Cerullo, and R. Osellame, "Three-dimensional Mach-Zehnder interferometer in a microfluidic chip for spatially-resolved label-free detection," *Lab Chip* **10**(9), 1167-1173 (2010).
28. M. J. Levene, J. Korlach, S. W. Turner, M. Foquet, H. G. Craighead, and W. W. Webb, "Zero-mode waveguides for single-molecule analysis at high concentrations," *Science* **299**(5607), 682–687 (2003).
29. B. B. Rosenblum, F. Oaks, S. Menchen, and B. Johnson, "Improved single-strand DNA sizing accuracy in capillary electrophoresis," *Nucleic Acids Res.* **25**(19), 3925–3929 (1997).
30. M. Kataoka, S. Inoue, K. Kajimoto, Y. Sinohara, and Y. Baba, "Usefulness of microchip electrophoresis for reliable analyses of nonstandard DNA samples and subsequent on-chip enzymatic digestion," *Eur. J. Biochem.* **271**(11), 2241–2247 (2004).
31. A. Minucci, G. Canu, M. De Bonis, E. Delibato, and E. Capoluongo, "Is capillary electrophoresis on microchip devices able to genotype uridine diphosphate glucuronosyltransferase 1A1 TATA-box polymorphisms?," *J. Sep. Sci.* **37**(12), 1521–1523 (2014).
32. B. M. Paegel, C. A. Emrich, G. J. Wedemayer, J. R. Scherer, and R. A. Mathies, "High throughput DANN sequencing with a microfabricated 96-lane capillary array electrophoresis bioprocessor," *Proc. Natl. Acad. Sci. USA* **99**(2), 574–579 (2002).
33. C. Dongre, J. van Weerd, G. A. Besselink, R. van Weeghel, R. M. Vazquez, R. Osellame, G. Cerullo, M. Cretich, M. Chiari, H. J. W. M. Hoekstra, and M. Pollnau "High-resolution electrophoretic separation and integrated-waveguide excitation of fluorescent DNA molecules in a lab on a chip," *Electrophoresis* **31**(15), 2584–2588 (2010).
34. Lionix B.V., 2016. http://www.lionixbv.nl.
35. R. Osellame, H. J. W. M. Hoekstra, G. Cerullo, M. Pollnau, "Femtosecond laser microstructuring: an enabling tool for optofluidic lab-on-chips," *Laser Photonics Rev.* **5**(3), 442–463 (2011).
36. R. Osellame, S. Taccheo, M. Marangoni, R. Ramponi, P. Laporta, D. Polli, S. de Silvestri, and G. Cerullo, "Femtosecond laser writing of active optical waveguides with astigmatically shaped beams," *J. Opt. Soc. Am. B* **20**(7), 1559–1567 (2003).
37. M. Cretich, M. Chiari, G. Pirri, and A. Crippa, "Electroosmotic flow suppression in capillary electrophoresis: chemisorptions of trimethoxy silane-modified polydimethylacrylamide," *Electrophoresis* **26**(10), 1913–1919 (2005).

38. H. Tian and J. P. Landers, "Hydroxyethylcellulose as an effective polymer network for DNA analysis in uncoated glass microchips: optimization and application to mutation detection via heteroduplex analysis," *Anal. Biochem.* **309**(2), 212–223 (2002).
39. Capilix B.V., 2015. http://www.capilix.com.
40. L. Alaverdian, S. Alaverdian, O. Bilenko, I. Bogdanov, E. Filippova, D. Gavrilov, B. Gorbovitski, M. Gouzman, G. Gudkov, S. Domratchev, O. Kosobokova, N. Lifshitz, S. Luryi, V. Ruskovoloshin, A. Stepoukhovitch, M. Tcherevishnick, G. Tyshko, and V. Gorfinkel, "A family of novel DNA sequencing instruments based on single-photon detection," *Electrophoresis* **23**(16), 2804–2817 (2002).
41. C. Dongre, J. van Weerd, G. A. Besselink, R. M. Vazquez, R. Osellame, G. Cerullo, R. van Weeghel, H. H. van den Vlekkert, H. J. W. M. Hoekstra, and M. Pollnau, "Modulation-frequency encoded multi-color fluorescent DNA analysis in an optofluidic chip," *Lab Chip* **11**(4), 679–683 (2011).
42. A. M. Schrell and M. G. Roper, "Frequency-encoded laser-induced fluorescence for multiplexed detection in infrared-mediated quantitative PCR," *Analyst* **139**(11), 2695–2701 (2014).

1. Introduction

A lab on a chip [1–3] squeezes the functionalities of a biological or chemical laboratory onto a single substrate. Its advantages are speed of analysis, low reagent volumes, and measurement automation and standardization. Capillary electrophoresis (CE) is a powerful method for biomolecule separation and analysis [4–6]. The sorting and sizing of DNA molecules within the human genome project [7] has been enabled largely by CE separation and analysis [8] and has led to the genetic mapping of various human illnesses [9]. On-chip integration of DNA sequencing [10–13] and genetic diagnostics [14, 15] have become feasible. Laser-induced fluorescence exploiting fluorescent dye labels is the most popular microchip CE monitoring technique, allowing a low limit of detection of 210 fM [16].

Micro-optical components have been integrated in microfluidic labs on a chip to perform on-chip optical detection [17–27]. Integrated optical waveguides allow one to confine and transport light in the chip, directing it to a small volume of the microfluidic channel and collecting the emitted/transmitted light, as has recently been applied to monitor on-chip DNA sequencing [11, 28] in a now commercialized DNA sequencer [13].

Sizing accuracy poses an inherent challenge to CE and particularly microchip CE [29–31]. Application of CE-based DNA sequencing in a lab-on-a-chip to identify genomic deletions or insertions associated with genetic illnesses critically depends on the detection of single base-pair insertions or deletions from DNA fragments in the diagnostically relevant range of 150–1000 base-pairs, i.e., it requires a variance of $\sigma^2 < 10^{-3}$, while only $\sigma^2 < 10^{-2}$ were reported [32, 6, 33]. Here we test different calibration strategies and demonstrate CE-based DNA analysis in an optofluidic chip with sub-base-pair resolution ($\sigma^2 \approx 4\times10^{-4}$) of low concentrations of DNA molecules, thereby paving the way for the envisaged application.

2. Experimental

A schematic of the commercial microfluidic chip [34] is displayed in Fig. 1. The microfluidic channel network and reservoirs were patterned photolithographically and wet-etched in fused silica glass and then sealed off by bonding another piece of fused silica glass on top. The chip has dimensions of 55 mm × 5.5 mm × 1 mm and the microfluidic channels have a cross-section of ~110 µm width and ~50 µm depth. The optical waveguide was inscribed into the bulk of the fused silica chip by fs-laser writing [35] at a translation speed of 20 µm/s, using a Ti:Sapphire laser operating at 800 nm wavelength with 150 fs, 4 µJ pulses at a repetition rate of 1 kHz. Employing tunable, astigmatic beam shaping [36], an elliptical cross section of the written waveguide was obtained, with a major diameter of ~50 µm in the vertical direction, while the minor diameter in the horizontal direction is ~12 µm in order to retain a high spatial resolution along the direction of DNA migration and separation.

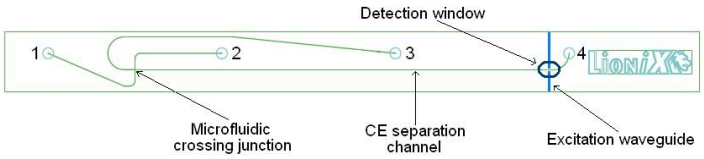

Fig. 1. Schematic of the optofluidic chip showing reservoirs 1–4, sample injection channel (reservoir 1 → reservoir 2) and CE separation channel (reservoir 3 → reservoir 4), as well as the integrated optical waveguide and detection window.

Prior to the experimental runs the inner walls of the microfluidic channel network were coated with an epoxy-poly-(dimethylacrylamide) (EPDMA)-based polymer [37]. Subsequently, the channels were filled with a sieving gel matrix consisting of hydroxyethyl-cellulose (HEC) (2% wt./vol.) [38], dissolved in 20 mM MES / 20 mM His buffer (pH 6.2). The reagents were sterilized, filtered (0.22 μm pore size), and stored at 269 K.

The CE sample loading and separation protocol was based on optimized actuation voltages of up to 1.5 kV, delivered by Pt electrodes integrated into the microfluidic reservoirs. The entire on-chip migration was controlled with a LabVIEW (National Instruments, Inc.) script steering a microfluidic control system [39]. Application of a high voltage forced the analyte molecules to migrate into the CE injection channel from sample reservoir 1 to waste reservoir 2 (see Fig. 1). By switching the voltages at all four reservoirs simultaneously a well-confined plug containing the mixture of analyte molecules – with a volume of ~605 picoliters at the crossing junction of the two microfluidic channels – was injected into the CE separation channel, from the microfluidic crossing junction toward waste reservoir 4, and the analyte molecules contained in the plug volume were separated according to their size. The excitation waveguide intersects the CE separation channel orthogonally at a distance of ~3.6 cm from the microfluidic crossing junction at which the separation commences, toward the end of the CE separation channel, close to reservoir 4, where the plug separation is highest.

Chip surfaces not required to transmit light were blackened to suppress reflections of parasitic light. A photon-counting photomultiplier tube (H7421-40, Hamamatsu) cooled to 203 K was built onto the output port of an inverted microscope (DM5000, Leica Microsystems) and aligned to collect the fluorescence signal through the detection window. Combination of excitation/emission band filters (K3, Leica Microsystems, and XF57, Omega Optical) in the fluorescence collection path ensured that only fluorescence signals emitted by labeled DNA molecules reached the photomultiplier tube, while other sources of background signal, including scattered laser light, were rejected. The fluorescence intensity, recorded as a function of time, was further numerically post-processed to obtain a high signal-to-noise ratio.

Two sets of DNA molecules with known base-pair sizes were covalently and permanently end-labeled with different dyes during a polymerase chain reaction. Previous attempts with intercalating dyes resulted in less good sizing accuracy than reported here for covalent dyes. In a single flow experiment, the 12 blue-labeled (Alexa fluor 488) and 23 red-labeled (Alexa fluor 647) DNA fragments were separated in size by microchip CE. Each set was excited exclusively by either of two lasers power-modulated at different frequencies of 17 Hz and 31 Hz and launched through the optical waveguide. The emitted and detected blue and red signals were distinguished by Fourier analysis. In this manner one can separate differently encoded fluorescence signals from each other [40–42]. The experiment was repeated with the same optofluidic chip without renewing the inner wall coating or sieving gel matrix.

3. Results and Discussion

The results of migration time of the 12 blue-labeled and 23 red-labeled DNA fragments versus DNA base-pair size for both experiments are displayed in Fig. 2(a) and 2(b). Rearrangement of these experimental data to compare separation of the same set of DNA

molecules in consecutive experiments, as displayed in Fig. 2(c) and 2(d), shows that the 12 blue-labeled DNA molecules in Fig. 2(c) exhibit less deviation of individual DNA molecules from the fitted temporal behavior than the 23 red-labeled DNA molecules in Fig. 2(d). It is also seen from Fig. 2(c) and 2(d) that the first experiment is better reproduced by the second one for the 12 blue-labeled molecules. We fitted the data of the logarithm of the base-pair size, S_{bp}, as a function of migration time, t, with a linear and a quadratic dependence,

$$\ln\left(S_{bp}\right) = a\,t + b\ , \tag{1}$$

$$\ln\left(S_{bp}\right) = c\,t^{2} + d\,t + e\ , \tag{2}$$

respectively. Table 1 provides the least-square fits of the experimental data of Fig. 2(c) and 2(d) according to Eqs. (1) and (2). Both figures show that a quadratic fit reproduces the measured data much better than a linear fit, indicating that the assumption of a simple logarithmic dependence of migration time on base-pair size underlying the production of DNA ladders with a logarithmic increase in base-pair size is not justified by our experiment.

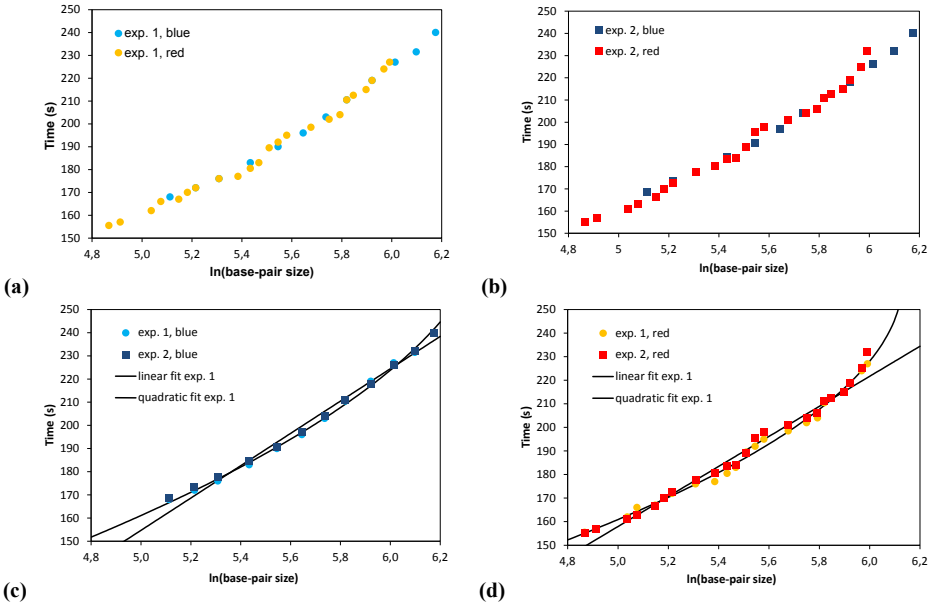

Fig. 2. Migration time (linear scale) versus base-pair size (logarithmic scale) of 12 blue-labeled (light and dark blue) and 23 red-labeled (orange and red) DNA molecules simultaneously migrated and separated in (a) experiment 1 ("exp. 1", circles) and (b) experiment 2 ("exp. 2", squares). The same data of (c) 12 blue-labeled and (d) 23 red-labeled DNA molecules. Linear and quadratic fits (solid lines) are shown only for the data of experiment 1.

Table 1. Parameters of the least-squares fits of the experimental data of Fig. 2(c) and 2(d) using the linear Eq. (1) or the quadratic Eq. (2).

Equation		Linear Eq.		Quadratic Eq.		
DNA label	Exp.	a [$\times 10^{-2}$]	b [$\times 1$]	c [$\times 10^{-5}$]	d [$\times 10^{-2}$]	e [$\times 10^{-1}$]
Blue	1	1.434	2.781	–7.599	4.520	–3.090
	2	1.471	2.700	–7.666	4.591	–4.345
Red	1	1.569	2.522	–10.899	5.727	–13.939
	2	1.517	2.605	–8.501	4.769	–4.627

In order to reach the goal of our investigation, the demonstration of sub-base-pair resolution during DNA separation in a simple optofluidic chip with high speed and low volume consumption, we tested different calibration strategies for the dependence of

migration time on base-pair size in a given experimental situation: a) use either set of DNA molecules as a reference to calibrate the set-up and identify the base-pair sizes of the other set in the same flow experiment, thereby eliminating variations in temperature, wall-coating and sieving-gel conditions, and actuation voltages; b) use the same molecular set as reference and sample (in a real-life experiment the reference set would be the healthy counter-part of an unknown, potentially malign sample set) with the same fluorescence label, flown in consecutive experiments; c) perform cross-experiments based on different molecular sets with different labels, flown in consecutive experiments; d) also self-calibration in the same experiment was analyzed. In the calibration procedure all base-pair sizes of the calibrating set contribute to the sizing accuracy at all base-pair sizes of the sample set, hence the sizing accuracy does not change significantly if the two sets have slightly different base-pair sizes.

The resulting variance σ^2, which quantifies the deviation of the sample data from the fit function obtained from the reference data, is given in Table 2 and displayed in Fig. 3 for both, the linear and quadratic fits from Fig. 2(c) and 2(d) for the four different approaches a)–d) proposed above. These results are obtained under the optimized experimental conditions described above. Variation of these conditions typically leads to less good sizing accuracy.

Table 2. Variance σ^2 [10^{-3}] using the linear Eq. (1) (italic numbers) or the quadratic Eq. (2) (bold numbers).

Variance σ^2 [10^{-3}]		Blue sample		Red sample	
		Exp. 1	Exp. 2	Exp. 1	Exp. 2
Blue ref.	Exp. 1	*1.595* **0.310**	*1.474* **0.242**	*3.719* **1.035**	*2.824* **1.343**
	Exp. 2	*1.674* **0.424**	*1.398* **0.133**	*3.305* **1.353**	*2.579* **1.903**
Red ref.	Exp. 1	*2.681* **1.582**	*1.952* **2.165**	*2.831* **0.716**	*2.610* **1.064**
	Exp. 2	*2.002* **1.145**	*1.521* **1.633**	*2.965* **0.913**	*2.467* **0.844**

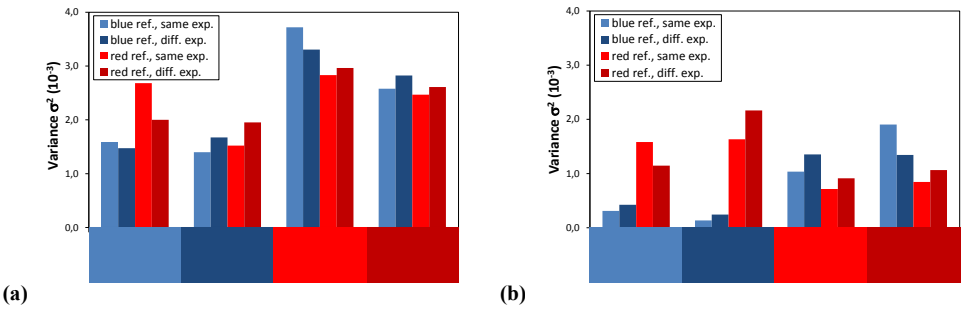

Fig. 3. Variance σ^2 of sample data measured in experiment ("exp.") 1 or 2 from (a) the linear fit function of Eq. (1) and (b) the quadratic fit function of Eq. (2), which were obtained from the measured reference ("ref.") data from the same or the different ("diff.") experiment.

From the experimental results (Fig. 2) and the analysis (Fig. 3) we conclude the following: 1) Applying a quadratic [Fig. 3(b)] instead of the usual linear [Fig. 3(a)] fit considerably improves the accuracy of calibration. 2) Blue-labeled molecules [Fig. 2(c)] are separated with higher accuracy than red-labeled molecules [Fig. 2(d)]; apparently, different dye labels influence the DNA flow differently. 3) In a laboratory environment, different dye labels affect the microfluidic flow of DNA plugs more severely than variations in temperature, wall-coating and sieving-gel conditions, and actuation voltages between consecutive experiments. 4) Choosing a single, suitable dye label (here: Alexa fluor 488), combined with reference calibration and sample investigation in consecutive experiments [left-hand side of dark-blue curve in Fig. 3(b)], results in a variance of $\sigma^2 = 4.2 \times 10^{-4}$ in one and $\sigma^2 = 2.4 \times 10^{-4}$ in the

opposite of two possible combinations of reference and sample, thereby demonstrating the feasibility of detecting single base-pair insertion/deletion in a lab-on-a-chip.

4. Summary

Choice of a suitable dye label, combined with reference calibration and sample investigation by fluorescent detection in consecutive experiments, results in capillary electrophoretic separation of fluorescent-labeled DNA molecules in the 150–1000 base-pair range with sub-base-pair resolution, thereby paving the way towards the detection of single base-pair insertion or deletion in a lab-on-a-chip with low reagent volumes in a few-minute experiment.

Funding

Deutsche Forschungsgemeinschaft DFG, project HA 7314/1-1.

Acknowledgments

The authors thank J. van Weerd and G.A.J. Besselink for their assistance in performing the electrophoresis experiments, H.H. van den Vlekkert for providing the lab-on-a-chip device, and R. Martinez Vazquez, R. Osellame, and G. Cerullo for the optical waveguide integration.